Mechanical Properties and Deformation Behavior of the Double Gyroid Phase in Unoriented Thermoplastic Elastomers

Benita J. Dair,[†] Christian C. Honeker,[†,||] David B. Alward,[†,⊥] Apostolos Avgeropoulos,[‡] Nikos Hadjichristidis,[‡] Lewis J. Fetters,[&] Malcolm Capel,[§] and Edwin L. Thomas*[,†]

Department of Materials Science and Engineering, Massachusetts Institute of Technology, Cambridge, Massachusetts 02139, Department of Chemistry, University of Athens, Panepistimiopolis, 157 71 Zougrafou, Athens, Greece, National Synchrotron Light Source, Brookhaven National Laboratory, Upton, New York 11973, and Corporate Research Science Lab, Exxon Research and Engineering Company, Clinton Township, Annandale, New Jersey 08801

Received April 29, 1999; Revised Manuscript Received August 12, 1999

ABSTRACT: The mechanical properties of the double gyroid (DG) cubic phase in glassy−rubbery block copolymer systems are examined. The stress−strain properties of an isoprene-rich polystyrene/polyisoprene/polystyrene (SIS) triblock and a polystyrene/polyisoprene (SI) starblock DG, both comprised of two separate interpenetrating glassy networks embedded in rubbery matrices, are compared to those of the sphere, cylinder, and lamellar morphologies. This 3-dimensionally interpenetrating periodic nanocomposite is found to have superior properties over those of its classical counterparts, attributable to the morphology rather than to the volume fraction of the glassy component, the architecture of the molecule, or the molecular weight. The DG is the only polygranular/isotropic thermoplastic elastomer morphology which exhibits necking and drawing and which requires considerably higher stresses for deformation up to 200% strain than any of the three classical microdomain morphologies. The deformation behavior of the DG is further investigated as a function of applied strain using in situ synchrotron small-angle X-ray scattering. Yielding and necking are observed at ∼20% strain, accompanied by sudden changes in the SAXS patterns: the characteristic Bragg rings of the DG disappear and are replaced by a lobe pattern containing streaks and diffuse scattering. Analysis of the {211} reflection in the SAXS data indicates that PS networks play a large role in governing the deformation behavior. The necking behavior of the DG suggests a different deformation mechanism. The DG samples recover both microscopically and macroscopically upon unloading and annealing, indicating that the complex interconnected nanocomposite structure was not permanently damaged, even after having been stretched to 600% strain.

Introduction

An A/B/A triblock copolymer consists of three macromolecules covalently bonded together. The self-assembly and microphase separation into A and B domains has been exploited by the thermoplastic elastomer industry for over 30 years.[1] A good historical account of the developments of triblock copolymers is given in refs 2 and 3. Triblock copolymers of the glassy−rubbery−glassy type with majority rubbery composition make mechanically useful elastomers, as both ends of the rubbery midblock are held fixed by the glassy phases, thereby creating a physically cross-linked model ordered nanocomposite system which is high-temperature melt-processable and recyclable. These materials can be considered very fine scale composites since the polystyrene (PS) and the polydiene microdomains still retain some of the character of their respective homopolymers. In particular, the material as a whole exhibits two glass transition temperatures characteristic of the two types of microdomains.[4−7]

The double gyroid phase was discovered in diblock copolymer systems[8,9] and more recently in triblock copolymers.[10−13] A schematic of two unit cells of the DG morphology is shown in Figure 1. This cubic microdomain morphology consists of a pair of 3-dimensionally continuous networks in a 3-dimensionally continuous matrix. We synthesized a PI-rich (66 vol % polyisoprene) SIS triblock copolymer of 74 000 total molar mass and block molecular weights of 14K−46K−14K. This molecular weight and composition is comparable to current commercial elastomeric materials, thereby allowing the exploration of new thermoplastic elastomer properties and applications. The calculated $\Delta N\chi$ from the critical $N\chi$ of about 40[14,15] places this triblock in the intermediate segregation regime where N is the number of statistical segments and χ is the Flory−Huggins segment−segment interaction parameter.

The reinforcing glassy PS component forms the two networks with the PS struts having L/D ratios of about ∼3:1.[16] Each PS network surrounds a skeletal graph of trifunctional interconnected nodes with each set of three coplanar struts successively twisted by 71° from one node to the next throughout space. The rubbery B-midblock chain forms a loop if its two A-end blocks are embedded in the same glassy network, whereas it forms a bridge if each A block belongs to a different network. The {211} planes have the highest PS density within the DG structure. The respective planes of highest glassy reinforcing phase density are the {001} planes

* To whom correspondence should be addressed.
[†] Massachusetts Institute of Technology.
[‡] University of Athens.
[§] Brookhaven National Laboratory.
[||] Present address: Max-Planck-Institut für Polymerforschung, Mainz, Germany.
[⊥] Present address: Solutia, Inc., Springfield, MA 01151.
[&] Exxon Research and Engineering Company.

10.1021/ma990666h CCC: $18.00
Published on Web 10/21/1999

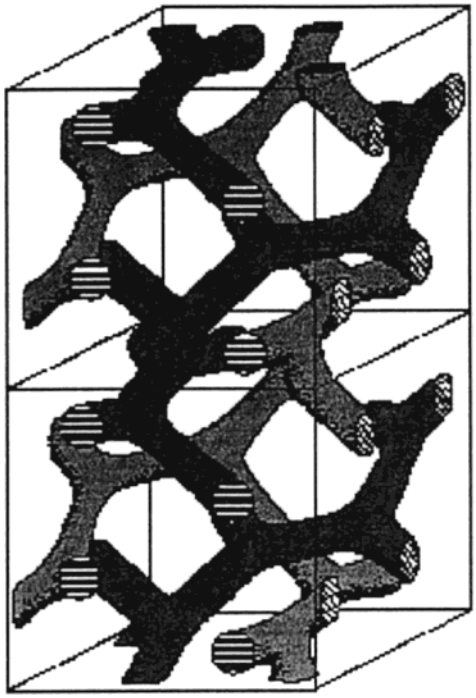

Figure 1. Schematic of the double gyroid morphology, shown with two unit cells. The two interpenetrating networks correspond to the PS domains in a matrix of PI.

in the lamellar and the {10} planes in the cylindrical structure.[17−19]

The mechanical behavior of elastomeric triblocks with the classical microdomain morphologies has been investigated extensively (for good reviews, see refs 2, 20, and 21). To date there have been some small-strain mechanical testing studies done on bicontinuous ordered morphologies,[22−24] and two preliminary conference reports by our group concerning the large strain deformation behavior of the DG microdomain structure.[25,26] In addition, the mechanical properties of a chaotic nonequilibrium bicontinuous morphology were also studied.[27]

The double gyroid morphology features 3-dimensionally periodic and interconnected structures: the two PS networks interpenetrate throughout space within a matrix of 3-dimensionally continuous PI. None of the classical phases have the reinforcing glassy phase continuous in all 3 dimensions. The classical spherical microdomain morphology consists of discrete PS spheres arranged on a body-centered cubic lattice, and the cylinder morphology consists of 1-dimensionally continuous PS rods arranged on a hexagonal lattice, both embedded in a PI matrix, while the lamellar morphology consists of alternating layers of PS and PI which are both continuous in two dimensions. The presence of the glassy reinforcing phase, continuous in all three dimensions in the DG structure may be expected to significantly affect the mechanical properties of the polymer.

In one of the earliest studies of block copolymer materials, Childers and Kraus[28] studied the mechanical properties of about 10 triblock SBS copolymers. Two of the copolymers they studied are within the composition range for DG (a morphology then unknown). Neither the equilibrium (simple cast) morphologies nor the stress−strain properties of these two polymers were investigated—the 34 wt % S was used in stress-relaxation studies only, and the 36% S was used in mineral-oil-extended studies only.

Alward et al.[22−24] studied the mechanical behavior of polystyrene-polyisoprene star block copolymers. These star block copolymers are 30 wt % PS and have diblocks as arms, connected by a multifunctional chlorosilane molecule. The microdomain structure of a series of star copolymer molecules with different arm numbers and different arm molecular weights, but with the same arm composition and overall composition, was found to depend on the number of arms. Stars composed of two, four, or five diblock arms had a cylinder morphology, while the 6-, 8-, 12- and 18-arm stars exhibited an ordered, 3-dimensionally bicontinuous structure, then called OBS (ordered bicontinuous structure). Dynamic mechanical thermal analysis (DMTA) results (shown in Figure 3 of ref 24) showed that the five-arm star (cylinder morphology) exhibited a room-temperature modulus of approximately 3 MPa, but the six-arm star (OBS morphology) exhibited a room-temperature modulus of approximately 20 MPa, about 1 order of magnitude higher than the cylinder-morphology star. The ordered bicontinuous structure was later shown to be DG.[29] The fact that the two samples have the same composition and only a 16% difference in total molecular weight indicated that the drastic change in the modulus is due to the difference in domain morphology.

The simplest deformation studies are those on solution-cast isotropic polygranular materials, as such materials require no special processing, and give insight into the general effects of morphology on stress−strain behavior. With this in mind, the stress−strain behavior of DG will be compared to that of the classical sphere, cylinder, and lamellar morphologies. Then results of in situ SAXS stretching experiments on the DG will be presented in an effort to follow the evolution of the microstructure during deformation.

Experimental Section

Table 1 lists the molecular characteristics of the classical microdomain structure and DG structure polymers studied. Synthesis of the SIS polymer having DG morphology is described elsewhere.[10] The sphere, cylinder, and lamellar morphology SIS polymers are commercially available from the Dexco company. The PS end block molecular mass lies between 11.5 and 18 kg/mol in each case, all well below the critical molecular weight for viscous entanglement for PS homopolymer (M_c^{PS} = 31 kg/mol). The PI midblock molecular mass ranges from 44 to 105 kg/mol, well above the critical molecular weight for viscous entanglement for PI homopolymer (M_c^{PI} = 14 kg/mol). The different morphologies are realized by changing the percent PS content, and all samples studied have majority PI composition. Synthesis of the two custom star block copolymers is also described elsewhere.[23] These materials have diblocks as arms, with the diblock composition listed in Table 1. The two-arm star is thus a triblock, also with the PI midblock well above M_c^{PI} and PS end blocks below M_c^{PS}.

All tensile samples were prepared using the same procedures. Polycrystalline isotropic, unoriented films 1.0 mm thick were cast from a dilute solution (∼5 wt %) with a nonselective solvent (toluene) into glass crucibles and the solvent allowed to slowly evaporate over a period of 2 weeks at ambient conditions. Irganox stabilizer was added at <0.25 wt % to the solution in order to prevent oxidation of the isoprene double bond when annealed at 120 °C. Films were easily removed from the glass crucibles by submerging the crucible in liquid nitrogen and quickly pushing out the hardened disk. The polymer films were dried for 2 days under vacuum at room temperature and were subsequently annealed at 120 °C for 10 days under vacuum to promote long range order and equilibrium microstructure. Typical grain sizes ranged from approximately 0.5 to 1 μm. Tensile samples 1.5 mm wide × 15 mm long were cut from the 1 mm thick films.

Table 1. Characteristics of the Polymers Studied

(a) Thermoplastic Elastomer Triblocks

morphology of triblock TPEs	total weight percent PS	total molecular mass (kg/mol)	block molecular masses (kg/mol) PS/PI/PS	polydispersity	source
spheres "SPH"	18% S	128	11.5/105/11.5	1.03	Dexco Vector 4111D
cylinders "CYL"	30% S	97	14.5/68/14.5	1.03	Dexco Vector 4211D
double gyroid "DG"	36% S	74	13.6/46.4/13.6	1.04	custom[10]
lamellae "LAM"	45% S	80	18/44/18	1.03	Dexco Vector 4411D

(b) Starblock Copolymers

morphology of starblocks	total weight percent PS	total molecular mass (kg/mol)	average functionality of star (PDI)	source
diblock precursor	30% S	33	1.04	custom[23]
DG (12-arm star)	30% S	396	11.7	custom[23]
cylinder (2-arm star)	30% S	66	2	custom[23]

The X-ray diffraction (SAXS) data were acquired at the Time-Resolved Diffraction Facility (station X12B) at the National Synchrotron Light Source at Brookhaven National Laboratory (BNL).[30] The optical system provides a doubly focused (spot size, 0.5 × 0.5 mm fwhm) monochromatic X-ray beam with a wavelength of $\lambda = 1.54$ Å. Sample-to-detector distances ranged from 215 to 260 cm. A tensile stage with an attached load cell was used to deform tensile specimens at strain rates of approximately 0.012 s^{-1}. SAXS patterns, along with simultaneous load−deformation curves, were taken as tensile specimens were loaded up to 600% and unloaded to zero load. Scattering patterns were collected during the deformation using a custom-built two-dimensional gas-delay line detector (10 × 10 cm, 512 × 512 pixels)[31] with exposure times of about 15 s.

SAXS data are represented by plots of scattered intensity as a function of the scattering vector q, which is defined as $q = 4\pi(\sin\theta)/\lambda$, where θ is half of the scattering angle 2θ, and λ is the wavelength of the X-rays. Using this relation and Bragg's law for scattering, the spacing of the scattering hkl planes, d_{hkl}, are related to the scattering vector by $d_{hkl} = 2\pi/q_{hkl}$.

Results and Discussion

Mechanical Properties and Stress−Strain Behavior. Parts a and b of Figure 2 show the stress−strain curve of polygranular isotropic double gyroid SIS triblock copolymer along with data from polygranular isotropic SIS triblock copolymers of the three classical phases, whose different microdomain morphologies are realized by changing PS content. Figure 2a shows the data out to 600% strain, and Figure 2b is an enlargement of the 0−100% strain region. Table 2 lists the mechanical properties of the various morphologies. Although the shapes of the stress−strain curves of the different samples have different characters, the modulus systematically increases with increasing PS content, in accordance with a reinforcing filler effect. The most prominent features of the curves are that the DG sample exhibits a stable neck, as can be discerned through the drop in load in the stress−strain curve and also visually on the sample itself, whereas the sphere, cylinder, and even the lamellar microdomain samples do not exhibit necking. (Necking is an inhomogeneous yielding phenomenon where a condition of maximum load is followed by nonuniform or localized deformation.[32]) Two outstanding features of the DG stress−strain curve are that the yield stress of the double gyroid sample is much higher than that of even the higher PS content lamellar sample, and the DG material exhibits the highest stress levels up to ∼200% strain. The sphere and cylinder samples show a rubbery response with very broad and diffuse yielding with no distinct yield point. The lamellar sample yields, but necking and drawing phenomena are absent, as can be observed visually on the sample and from the shape of the stress−strain curve.

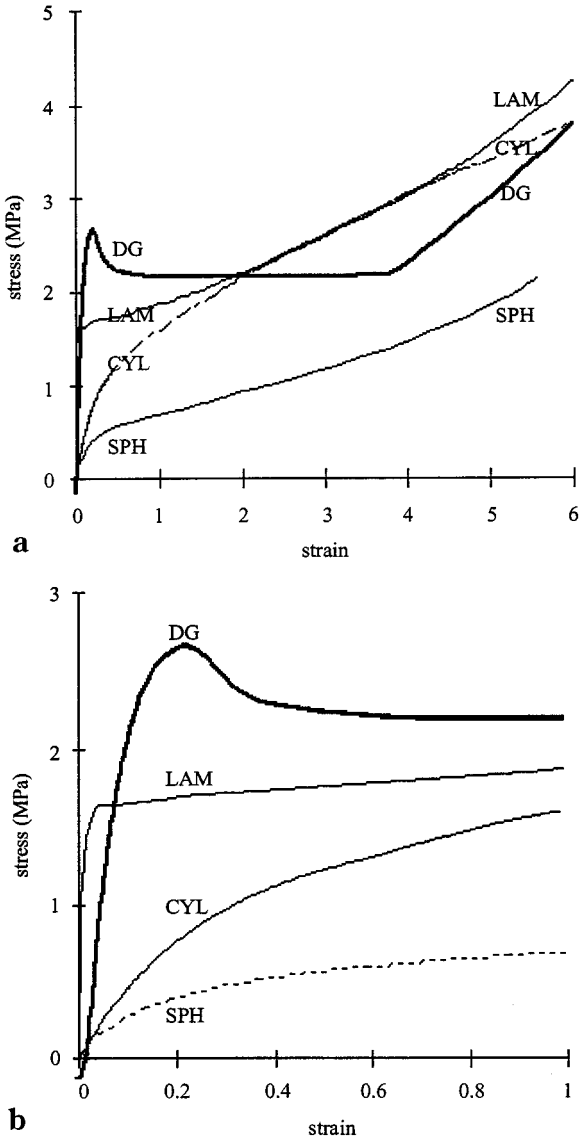

Figure 2. Stress−strain curves of isotropic, polygranular DG (bold), overlayed with the classical microdomain morphologies of spheres (SPH), cylinders (CYL), and lamellae (LAM). Key: (a) stress−strain behavior to 600% strain; (b) magnified portion of the stress−strain curve focusing on the 0−100% strain region.

Table 2. Mechanical Properties of Unoriented Elastomeric SIS Triblock Copolymer Morphologies[a]

morphology	modulus (MPa)	neck?	yield stress (MPa)	yield strain
	Triblocks			
spheres	2.5	no	n/a	n/a
cylinders	5	no	n/a	n/a
double gyroid	30−35	yes	2.6	0.20
lamellae	140−150	no	1.6	0.04
	Starblocks			
DG (12-arm star)	25−30	yes	1.3	0.10
cylinder (2-arm star)	3	no	n/a	n/a

[a] For the DG samples, the yield point on the stress−strain curve was taken as the point of maximum load. For the lamellar sample, the yield was taken as the point where the stress−strain curve abruptly bends over. Yield point determination for the sphere and cylinder samples was not applicable, as any yielding was diffuse and the slopes of the curves were continuously changing.

Both the stress−strain curve in Figure 2 and visual inspection of carefully prepared polygranular isotropic samples with lamellar microdomain morphology reproducibly indicate that the polygranular isotropic lamellar samples do not undergo necking and drawing phenomenon. Other studies in the literature also support this view.[33−36] Segula and Prud'homme do, however, report necking in a polygranular solvent cast lamellar sample containing 29 wt % polystyrene.[37,38] Samples with orientation or texture, often produced by various types of processing, sometimes undergo necking depending on the relative orientation of the applied force to the axes of continuous PS domains.[4,28,39−41]

As is mentioned in refs 2 and 20, necking is characteristic of continuous PS domains; i.e., necking in glassy/rubbery systems has been observed to occur when the glassy phase is continuous in the loading direction. In unoriented polycrystalline samples, the fact that necking *is* observed in the 36 wt % styrene (DG) sample and *not* in a 45 wt % styrene (lamellar) sample is surprising, because with increasing PS content, there is a higher probability that there exist some continuous PS paths in the direction of loading and hence a higher possibility of necking phenomenon. The fact that the samples of other microdomain morphologies with PS contents smaller (cylinders) as well as greater (lamellar) than the DG composition do not neck indicates that, in samples where PS is the minority component, necking is much more affected by the microdomain structure than by the PS content.

Figure 3 shows the stress−strain behavior of starblock copolymers whose different morphologies are realized by changing the number of diblock arms at constant PS composition.[23] The 12-arm starblock copolymer has the OBS/DG morphology[23,29] while the two-arm starblock copolymer (i.e., a triblock) has the cylinder morphology. Here again the OBS/DG phase exhibits necking and drawing phenomena, while the cylinder phase exhibits diffuse yielding without necking. The stress required to deform the samples to a given stress is higher for the OBS phase than for the cylinder phase at all strains shown.

Both Figures 2 and 3 demonstrate that the DG microstructure exhibits a more robust character than that of the cylindrical or lamellar structure, requiring higher stresses to deform to a given strain and yielding via stable necking behavior. The evidence presented here shows that the enhancement of mechanical properties of the DG samples over that of the classical

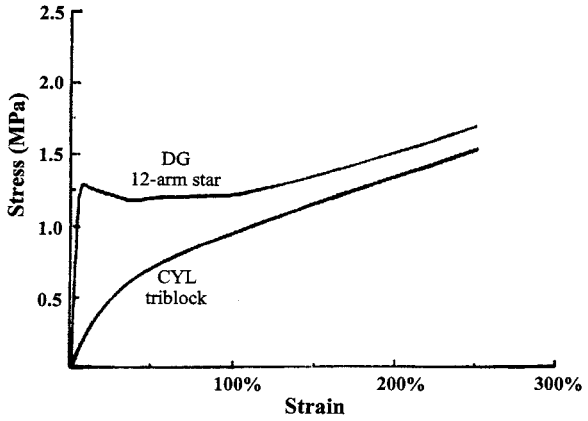

Figure 3. Stress−strain behavior of a isotropic, polygranular triblock having the cylinder phase and a starblock copolymer having the OBS/DG phase. Note that the OBS/DG phase exhibits yielding and necking phenomenon, but that the cylinder phase does not.

morphology samples is not an effect of percent PS content, architecture, or molecular weight (shown in ref 24). Hence, the enhancement in mechanical properties is essentially due to the unique 3D microdomain morphology of the double gyroid phase.

Evolution of Microdomain Structure with Deformation. Figure 4A shows a typical stress−strain curve of DG, with accompanying SAXS patterns recorded at different points along the deformation. The tensile modulus is approximately 30 MPa. Yield occurs at approximately 20% strain and approximately 2.6 MPa, accompanied by formation of a distinct neck. The hysteresis in the stress−strain curve is approximately 50%, and a Mullins effect is observed. As mentioned in refs 2 and 20, necking, hysteresis, and a Mullins effect suggest a slow recovery of the plastically deformed PS domains.

The SAXS pattern before the deformation begins is shown in Figure 4B and consists of an isotropic ring pattern with the characteristic {211} and {220} reflections of the double gyroid. Upon loading, the higher order Bragg rings fade, and the remaining innermost diffraction rings become elliptical. As a cubic structure, the DG is expected to exhibit mechanical anisotropy.[42] Therefore, in a collection of randomly oriented grains, the strain response will be different in each grain depending on the specific orientation to the force axis. Grains having continuous PS paths oriented in the direction of the applied force will deform less than those grains having such paths oriented transverse to the applied force. This anisotropy of grains provides an impetus for studying oriented DG more in depth in order to sample and elucidate the mechanisms for anisotropic deformation.[43−45]

At ∼20% strain, necking occurs, as indicated by the drop in the engineering stress − strain curve, by visual detection of a local region of much reduced sample cross-sectional area, and by the abrupt change in the nature of the scattering pattern (for the X-ray beam directly incident on the necking area), as shown by Figure 4C. The characteristic isotropic rings are much reduced in intensity, there is an increase in diffuse low angle scattering, and a pair of horizontal streaks oriented along the normal to the stretching direction appears. Upon further elongation, the ring completely disappears, and only the diffuse scatter and streaks remain, as in Figure 4D and schematically illustrated in Figure

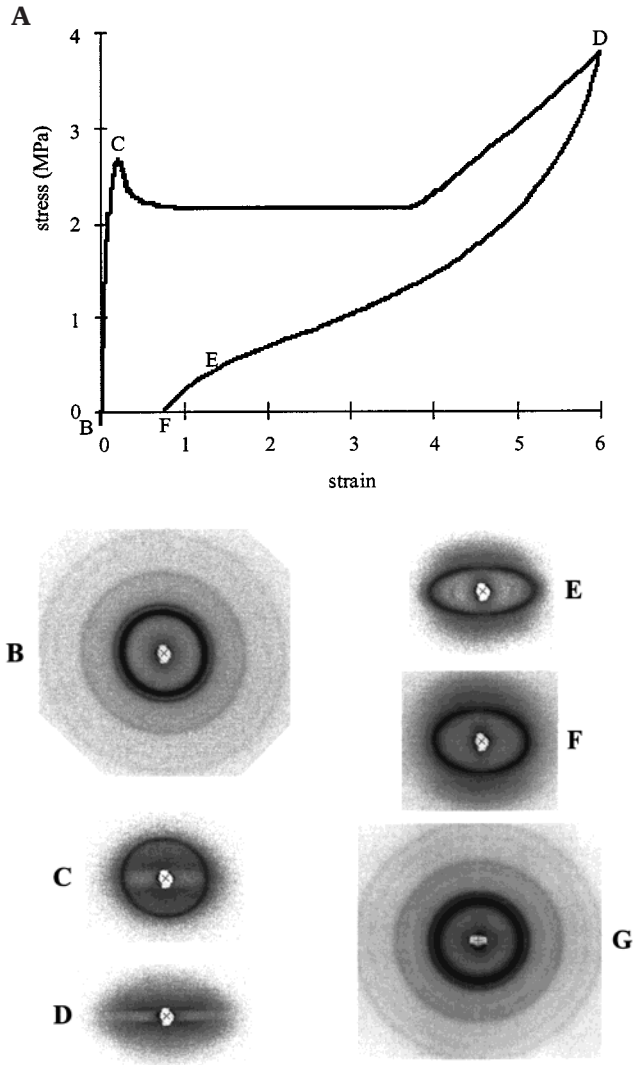

Figure 4. (A) Stress−strain curve of an isotropic, polygranular 34% S SIS DG (top), with accompanying SAXS patterns. (B) Pattern at start before deformation. (C) Pattern at yield, ∼20% strain. (D) Pattern at 600% strain. (E) Pattern unloaded to ∼130% strain. (E) Pattern fully unloaded, with ∼70% residual strain. (G) Pattern upon annealing at 120 °C for 2 weeks.

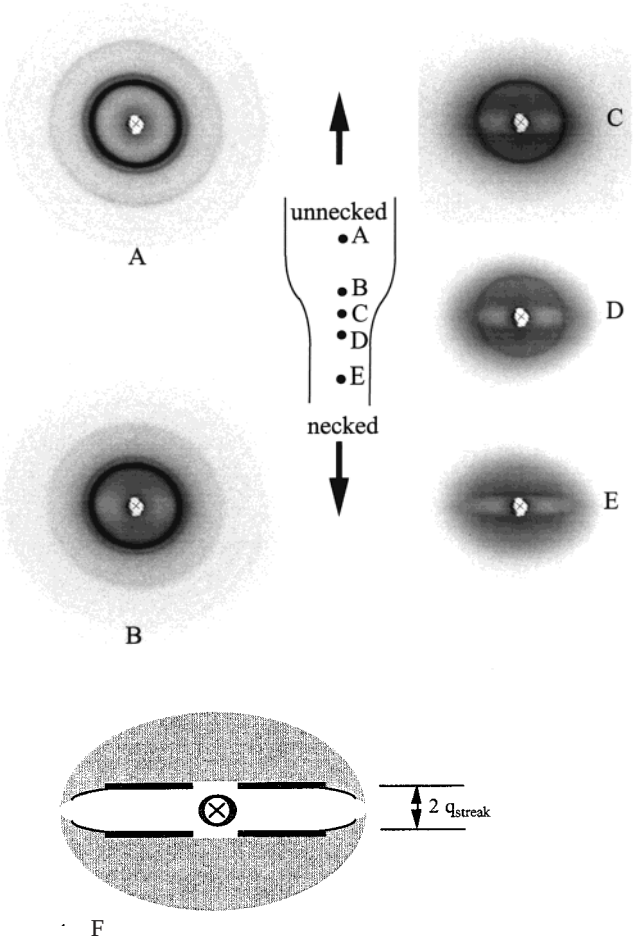

Figure 5. (A−E) Isotropic 34% S SIS DG sample loaded to 40% total strain capturing the necking transition (schematic shown center), with SAXS patterns of different points along the neck transition. Point A is closest to the unnecked material, while point E is in the necked region where the local strain is approximately 300−375%. (F) Schematic of a streak pattern characteristic of a necked specimen, like as shown in Figure 5E. The streak spacing is taken as the inverse of the distance along the direction of the applied force between the origin and the extended streak.

5F. This anisotropic scattering pattern does not change until the neck has propagated across the entire gauge length of the sample. Once the neck has encompassed the entire gauge length, the strain within the yielded material begins to increase. The streaks in the pattern become somewhat sharper and more elongated and move to lower q, but the nature of the pattern does not change.

The SAXS pattern shown in Figure 4C captures the sample morphology just in the abrupt transition from rings to streaks and shows the nearly circular ring of yet-unyielded material superposed on the diffuse scattering and horizontal streaks. Before continuing with the discussion of parts E−G of Figure 4, which show SAXS patterns for unloading the sample after large strain deformation, it is instructive to further probe the yielding phenomenon by stepping the X-ray beam across the neck region. To achieve this, a sample was stretched until a neck formed and propagated partially along the sample (nominal strain ∼50%).

The series of SAXS patterns taken along the transition from unnecked material to the necked material is depicted in Figure 5. Note that, in the unnecked region in Figure 5A, the sample pattern still consists of essentially circular rings, but as the necked region is approached, there are fewer higher order rings in the pattern (e.g., Figure 5B), and the remaining rings have become slightly elliptical. The ellipses are characteristic of a small strain (<5%) in the sample volume which is not large enough to cause yielding. In experiments where the sample is continuously stretched and where 5−10 s duration SAXS patterns are taken in rapid succession, it is also noticed that before necking the rings become elliptical, but at the moment when a neck is formed in another part of the sample, the rings in unyielded areas revert to circular as the strain in the unyielded area has been relieved by that in the localized deformation region.

Parts C and D of Figure 5 show that, in the region of the sample where the unnecked material transitions to necked material, the rings fade out in conjunction with development of the streak pattern. This indicates that there are regions of yielded material coexisting with regions of unyielded material.

From Considere's criterion for necking behavior, a material necks when the yield stress is equal to, or

exceeds, the strain hardening rate; i.e., if the relation $d\sigma/d\epsilon = \sigma$ is satisfied.[46−48] Or, if strain is expressed as the fractional change in area, the onset of necking occurs when the fractional change in yield stress is balanced by the fractional decrease in load bearing area $d\sigma/\sigma = -dA/A$. Strain hardening is the phenomenon where the stress increment required to strain the sample a given amount continuously increases with increasing strain. Materials which are prone to necking are those with a large yield stress but with low strain hardening rates. Polymeric materials generally exhibit *stable* necking, whereby the neck propagates across the entire sample with increasing strain, as opposed to metallic materials, which can neck unstably by thinning down until rupture occurs.[46] As necking in styrene−isoprene materials is associated with continuous PS domains, perhaps the relative magnitudes of the flow stress and strain hardening rate could primarily be associated with deformation of the PS domains. When a large amount of the displacement is carried by the PS, then the deformed area may strain harden quickly from the plastic deformation of the PS.

The isotropic polygranular cylindrical microdomain structure does not neck but yields diffusely, indicating that the yield stress is relatively lower than its strain hardening rate. This may be due to the grain structure. In the cylindrical microdomain morphology, the PS domains are likely to be discontinuous across certain types of grain boundaries,[49] thereby decreasing the sample yield stress. In addition, there are domains which are oriented such that glassy and rubbery domains are loaded in series, allowing the PI matrix to carry the deformation without simultaneously deforming the PS cylinders. The grains which are most compliant are those which have the PS cylinders oriented perpendicular to the direction of stretch, and those which are most resistant to deformation are those in which the glassy cylinders are oriented parallel to the direction of stretch. This is directly reflected in the large anisotropy in Young's modulus of 100−120× between parallel and perpendicular stretching in well-aligned near-single-crystal texture samples.[50,51] In a polygranular cylindrical sample, grains oriented in different directions will yield at different strains, giving rise to an overall diffuse yielding with the stresses low enough such that the strain hardening rate in the grains at those levels of stress is sufficient to prohibit the deforming material from developing a neck.

The lamellar microdomain structure also does not neck, but it does exhibit a distinct yield point. The sharp yielding in the case of the lamellar microdomain structure indicates that grains oriented in different directions may deform cooperatively or simultaneously throughout, which may be due to the considerably smaller anisotropy in Young's modulus of only 3× between parallel and perpendicular stretching of near-single-crystal texture samples.[39] In addition, the glassy PS domains are known to be continuous across the various types of grain boundaries of the lamellar morphology.[52,53] The absence of necking may be due to a high strain-hardening rate arising from the microdomain geometry (rubber layers confined between glassy layers), where deformation of the PS must occur when stretching perpendicular or parallel to the lamellae sheets[39] and where the PI, having a high bulk modulus, has a high resistance to shearing. The lamellae can then strain harden sufficiently such that the area which undergoes yield is able to withstand the current load, and neither a load drop nor localization of deformation occurs.

The PS domains are continuous across grain boundaries in the double gyroid morphology.[43] In addition, the 3D continuity of the PS networks raises the yield stress of the sample as a whole, since all directions in the material are reinforced with PS domains. The anisotropy of Young's modulus of the DG is approximately 5× with the highest modulus along the PS-continuous paths (⟨111⟩ directions) and the lowest along the transverse directions.[43,54] Therefore, the stress required for yield remains high no matter the grain orientation. The strain-hardening rate would be expected to be high because of the 3-D interconnectedness of the PS networks, where the PS struts must deform as the PI matrix is deformed. However, after yield, the DG structure does not exhibit as high a strain-hardening rate as that of a lamellar microdomain structure because there is less constraint on the PI by the networks of PS. When yield is reached, the strain hardening of the yielded area cannot withstand the current stress level, causing the load to drop and the strain to be localized within the yielded region. The yielded regions are sufficiently strain-hardened that the level of stress deforms adjacent unyielded material, drawing the unyielded material into the neck.

The strain in the necked region can be estimated several ways. The first is through measurements of the dimensions of the physical neck by the relation $\epsilon = \Delta L/L_o = A_o/A$, assuming no change in the sample volume upon deformation. The samples usually have initial cross-sections of 1−2 mm^2. Measurements from photographs of the neck show that the strain in the necked region is 350−400%. The other measure of the strain in the neck is that value at which the stress begins to rise after the drawing stress plateau. The strain in the neck is characteristic of the polymer's natural draw ratio and only when all of the sample has the same value of strain will the stress once again rise in the sample. When the neck has propagated across the entire gauge length, the strain is the same at all points, and macroscopic elongation of the sample results in an increase in strain uniformly throughout the sample. Therefore, the strain at which the stress just begins to rise after the plateau is the strain which is characteristic of the neck. Examination of the stress−strain curve in Figure 4 suggests a necking strain of about 375%.

A characteristic spacing was determined from the distance from origin to the center of the streak along the applied force direction as denoted in Figure 5F. At yield, the streak had an associated spacing of $d_{\text{yield}}^{\text{neck}} \approx$ 1200 Å. If this spacing is compared to the characteristic d_{211} of the simple cast DG, then the strain, $\epsilon = d_{\text{yield}}^{\text{neck}}/d_{211} - 1$, is approximately 360%, which is about the same necking strain determined previously. This is the first indication that the {211} reflection, which arises from planes of the highest PS content, allows insight into the deformation process.

The strain in a sample with 600% deformation was also determined from the origin-to-streak distance in Figure 4D. The streak corresponded to a spacing $d_{600\%} \approx$ 1800 Å. The calculated strain is $\epsilon = d_{600\%}/d_{211} - 1 =$ 700%, which is again approximately the macroscopically measured strain. Hence we find a strong correlation of the streak spacing to the amount of strain in the (211) planes of a yielded sample.

Figure 4E shows that, upon unloading, elliptical Bragg rings appear, starting at approximately 300% strain. Upon complete unloading, the sample shown has a nominal 70% residual axial strain determined from physical dimensions. Measurements from the elliptical ring pattern in Figure 4F indicate that there remains +40% strain in the axial direction and −20% strain in the transverse direction after unloading. This disparity is likely due to sample relaxation between the time when the nominal strain at zero load was measured and the time when the SAXS pattern was taken. The SAXS pattern of the stretched sample reannealed for 5 days at $T = 120°$ in Figure 4G is essentially identical to the original pattern in Figure 4B. The dimensions of the stretched and reannealed sample return to those of the original prestretched state. This indicates that any mode of large strain deformation is fully recoverable upon annealing.

Detailed Deformation Mechanisms Needed. The sudden change in the SAXS pattern coinciding with the onset of necking indicates a drastic structural change occurs. As was previously mentioned, necking and drawing phenomena in thermoplastic elastomers are characteristic of samples with continuous PS domains.[2,20] The extreme change in the nature of the SAXS patterns in Figure 4D and Figure 5C−E may indicate disruption of PS domains via yielding, rupture, or drawing of the PS networks. Because the deformation behavior of an isotropic polygranular sample is a superposition of the various responses of grains in different orientations, and because the SAXS patterns of the highly deformed sample consists of diffuse scattering and a pair of streaks, detailed modeling of the microstructural evolution during the deformation is difficult. Cubic materials can have an inherent mechanical anisotropy due to structural differences of the material in different directions, which would become apparent in a textured or oriented sample. Such structural differences should affect the large strain deformation mechanisms of the DG along different directions. Therefore, to elucidate the mechanical anisotropy and to observe if the deformation of the DG is directionally dependent, the mechanical behavior of oriented or textured materials needs to be studied. In fact, the mechanical properties and deformation behavior of oriented polymeric materials have been studied extensively[21,36,39,50,55−68] to understand the directional dependence of the mechanical properties and deformation behavior and to elucidate the elastic constants. In a forthcoming paper, the deformation of oriented DG will be presented in order to shed more light on the deformation mechanisms of this complex interconnected nanocomposite structure.[45]

Conclusions

The initial modulus of an isotropic polygranular DG SIS triblock is 30−35 MPa, and the yield stress is approximately 2.6 MPa, with yield occurring at 20% strain. The DG is the only PI-rich morphology which, when processed to have polygranular unoriented domains, necks and draws. The presence of the stable necking phenomenon is one indication that the DG structure is mechanically more robust than the classical morphologies, requiring higher stresses for yield than for the classical morphologies. This can be attributed to the specific DG microdomain geometry rather than the PS content, molecular architecture, or molecular weight. Necking in the DG sample is accompanied by a sudden change of the SAXS patterns from characteristic Bragg rings of an isotropic material to a pattern with diffuse low angle scatter and a pair of horizontal streaks. The strain in the necked region is about 350−400%. The streaks in the lobe pattern are associated with the highest-PS-density {211} planes of the DG, thereby suggesting that the {211} planes play a significant role in the deformation mechanism of this three-dimensional interconnected nanocomposite. Upon unloading, elliptical rings appear at 300% strain, and an immediate residual strain of 70% remains at zero load. Upon annealing, the sample returns to its original macroscopic and microscopic dimensions, indicating full recovery of the PS domains.

Acknowledgment. We would like to thank Prof. Yachin Cohen, Prof. Mary Boyce and Prof. Ali Argon for scientific discussion. This research was supported by the Air Force (AFOSR F49620-97-1-0385) and by the National Science Foundation (NSF DMR 98-07591).

References and Notes

(1) Legge, N. R. *Rubber Chem. Technol.* **1989**, *62*, 529−547.
(2) Holden, G.; Legge, N. R. In *Thermoplastic Elastomers*; 2nd ed.; Holden, G., Legge, N. R., Quirk, R. P., Schroeder, H. E., Eds.; Hanser Publishers: New York, 1996; pp 48−69.
(3) Molau, G. E. In *Block Polymers*; Aggarwal, S. L., Ed.; Plenum Press: New York, 1970; pp 79−106.
(4) Holden, G.; Bishop, E. T.; Legge, N. R. *J. Polym. Sci., Part C* **1969**, *26*, 37−57.
(5) Kraus, G.; Childers, C. W.; Gruver, J. T. *J. Appl. Polym. Sci.* **1967**, *11*, 1581−1591.
(6) Hendus, H.; Illers, K.-H.; Ropte, E. *Colloid Polym. Sci.* **1966**, *216−217*, 110−119.
(7) Beecher, J. F.; Marker, L.; Bradford, R. D.; Aggarwal, S. L. *J. Polym. Sci., Part C* **1969**, *26*, 117−134.
(8) Hajduk, D. A.; Harper, P. E.; Gruner, S. M.; Honeker, C. C.; Kim, G.; Thomas, E. L.; Fetters, L. J. *Macromolecules* **1994**, *27*, 4063−4075.
(9) Schulz, M. F.; Bates, F. S.; Almdal, K.; Mortensen, K. *Phys. Rev. Lett.* **1994**, *73*, 86−89.
(10) Avgeropoulos, A.; Dair, B. J.; Hadjichristidis, N.; Thomas, E. L. *Macromolecules* **1997**, *30*, 5634−5642.
(11) Laurer, J. H.; Hajduk, D. A.; Fung, J. C.; Sedat, J. W.; Smith, S. D.; Gruner, S. M.; Agard, D. A.; Spontak, R. J. *Macromolecules* **1997**, *30*, 3938.
(12) Avgeropoulos, A.; Chan, V. Z.-H.; Lee, V. L.; Ngo, D.; Miller, R. D.; Hadjichristidis, N.; Thomas, E. L. *Chem. Mater.* **1998**, *10*, 2109−2115.
(13) Matsushita, Y.; Suzuki, J.; Seki, M. *Phys. B, Condens. Matter* **1998**, *248*, 238.
(14) Owens, J. N.; Gancarz, I. S.; Koberstein, J. T.; Russell, T. P. *Macromolecules* **1989**, *22*, 3380−3387.
(15) Mayes, A. M.; Olvera de la Cruz, M. *J. Chem. Phys.* **1989**, *91*, 7228−7235.
(16) Grosse-Brauckmann, K. *J. Colloid Interface Sci.* **1997**, *187*, 418−428.
(17) Rançon, Y.; Charvolin, J. *J. Phys. Chem.* **1988**, *92*, 2646−2651.
(18) Delacroix, H.; Mariani, P.; Gulik-Krzywicki, T. *Colloq. Phys.* **1990**, *C7*, C7-119−C117-129.
(19) Delacroix, H.; Gulik-Krzywicki, T.; Mariani, P.; Risler, J.-L. *Liq. Cryst.* **1993**, *15*, 605−625.
(20) Quirk, R. P.; Morton, M. In *Thermoplastic Elastomers*; 2nd ed.; Hanser Publishers: New York, 1996; pp 72−100.
(21) Honeker, C. C.; Thomas, E. L. *Chem. Mater.* **1996**, *8*, 1702−1714.
(22) Alward, D. B. Ph.D. Thesis; University of Massachusetts: 1985.
(23) Alward, D. B.; Kinning, D. J.; Thomas, E. L.; Fetters, L. J. *Macromolecules* **1986**, *19*, 215−224.
(24) Kinning, D. J.; Thomas, E. L.; Alward, D. B.; Fetters, L. J.; Handlin, D. L. J. *Macromolecules* **1986**, *19*, 1288−1290.

(25) Dair, B. J.; Prasman, E.; Capel, M.; Thomas, E. L. In *Proceedings of the 10th Churchill Conference on the Deformation, Yield, and Fracture of Polymers*; Institute of Materials: Cambridge, England, 1997.
(26) Dair, B. J.; Thomas, E. L.; Avgeropoulos, A.; Hadjichristidis, N.; Capel, M. Presented at the International Symposium on Toughening of Plastics, August 1998 National Meeting of the American Chemical Society, Boston, MA, 1998.
(27) Sakurai, S.; Sakamoto, J.; Shibayama, M.; Nomura, S. *Macromolecules* **1993**, *26*, 3351−3356.
(28) Childers, C. W.; Kraus, G. *Rubber Chem. Technol.* **1967**, *40*, 1183−1199.
(29) Hajduk, D. A.; Harper, P. E.; Gruner, S. M.; Honeker, C. C.; Thomas, E. L.; Fetters, L. J. *Macromolecules* **1995**, *28*, 2570−2573.
(30) Capel, M. *Synchrotron Radiat. News* **1993**, *6*, 22−27.
(31) Capel, M. C.; Smith, G. C.; Yu, B. *Rev. Sci. Instrum.* **1995**, *66*, 2295−2299.
(32) McClintock, F. A.; Argon, A. S. *Mechanical Behavior of Materials*; Addison-Wesley: Reading, MA, 1966.
(33) Henderson, J. F.; Grundy, K. H.; Fischer, E. *J. Polym. Sci., Part C* **1968**, *16*, 3121−3131.
(34) Fischer, E.; Henderson, J. F. *J. Polym. Sci., Part C* **1969**, *26*, 149−160.
(35) Pedemonte, E.; Alfonso, G. C. *Macromolecules* **1975**, *8*, 85−86.
(36) Pedemonte, E.; Dondero, G.; Alfonso, G.; de Candia, F. *Polymer* **1975**, *16*, 531−538.
(37) Seguela, R.; Prud'homme, J. *Macromolecules* **1978**, *11*, 1007.
(38) Seguela, R.; Prud'homme, J. *Macromolecules* **1981**, *14*, 197−202.
(39) Fujimura, M.; Hashimoto, T.; Kawai, H. *Rubber Chem. Technol.* **1978**, *51*, 215−224.
(40) Hashimoto, T.; Fujimura, M.; Saijo, K.; Kawai, H.; Diamant, J.; Shen, M. In *Multiphase Polymers*; Cooper, S. L., Estes, G. M., Eds.; ACS Advances in Chemistry Series; American Chemical Society: Washington, DC, 1979; pp 257−275.
(41) Albalak, R.; Cohen, Y.; Dair, B. J.; Thomas, E. L. Manuscript in preparation.
(42) Nye, J. F. *Physical Properties of Crystals;* Clarendon Press: Oxford, England, 1957.
(43) Dair, B. J. Ph.D. Thesis, Massachusetts Institute of Technology, 1999.
(44) Dair, B. J.; Avgeropoulos, A.; Hadjichristidis, N.; Thomas, E. L. Manuscript in preparation.
(45) Dair, B. J.; Avgeropoulos, A.; Hadjichristidis, N.; Capel, M.; Thomas, E. L. Manuscript in preparation.
(46) Young, R. J.; Lovell, P. A. *Introduction to Polymers;* Chapman and Hall: New York, 1991.
(47) Courtney, T. A. *Mechanical Behavior of Materials;* McGraw-Hill, Inc.: New York, 1990.
(48) Dieter, G. E. *Mechanical Metallurgy*; McGraw-Hill: New York, 1986.
(49) Carvalho, B. L.; Lescanec, R. L.; Thomas, E. L. *Macromol. Symp.* **1995**, *98*, 1131−1146.
(50) Arridge, R. G. C.; Folkes, M. J. *J. Phys., Part D: Appl. Phys.* **1972**, *5*, 344−358.
(51) Honeker, C. C. Ph.D. Thesis, Massachusetts Institute of Technology, 1997.
(52) Gido, S. P.; Gunther, J.; Thomas, E. L.; Hoffman, D. *Macromolecules* **1993**, *26*, 4506−4520.
(53) Gido, S. P.; Thomas, E. L. *Macromolecules* **1994**, *27*, 6137−6144.
(54) Dair, B. J.; Avgeropoulos, A.; Hadjichristidis, N.; Thomas, E. L. Manuscript in preparation.
(55) Folkes, M. J.; Keller, A. *Polymer* **1971**, *12*, 222−236.
(56) Keller, A.; Dlugosz, J.; Folkes, M. J.; Pedemonte, E.; Scalisi, F. P.; Willmouth, F. M. *J. Phys. Colloq., C5a* **1971**, *32*, 295−300.
(57) Turturro, A.; Bianchi, U.; Pedemonte, E.; Ravetta, P. *Chim. Ind.* **1972**, *54*, 782−785.
(58) Pedemonte, E.; Turturro, A.; Dondero, G. *Br. Polym. J.* **1974**, *6*, 277−282.
(59) Odell, J. A.; Arridge, R. G. C.; Folkes, M. J.; Keller, A. *Polym. Prepr.* **1977**, *18*, 257−262.
(60) Odell, J. A.; Keller, A. *Polym. Eng. Sci.* **1977**, *17*, 544−559.
(61) Tarasov, S. G.; Tsvankin, D. Y.; Godovsky, Y. K. *Polym. Sci. USSR (Engl. Transl.)* **1978**, *20*, 1728−1739.
(62) Hadziioannou, G.; Mathis, A.; Skoulios, A. *Colloid Polym. Sci.* **1979**, *257*, 344−350.
(63) Hadziioannou, G.; Mathis, A.; Skoulios, A. *Colloid and Polymer Science* **1979**, *257*, 337−343.
(64) Schirrer, R.; Pixa, R. *Colloid and Polymer Science* **1980**, *258*, 802−806.
(65) Pakula, T.; Saijo, K.; Kawai, H.; Hashimoto, T. *Macromolecules* **1985**, *18*, 1294−1302.
(66) Allan, P.; Arridge, R. G. C.; Ehtaiatkar, F.; Folkes, M. J. *J. Phys. D* **1991**, *24*, 1381−1390.
(67) Yamaoka, I.; Kimura, M. *Polymer* **1993**, *34*, 4399−4409.
(68) Prasman, E.; Thomas, E. L. *J. Polym. Sci., Part B: Polym. Phys.* **1998**, *36*, 1625−1636.

MA990666H